Int. J. Heat Mass Transfer. Vol. 36, No. 3, pp. 611–616, 1993
Printed in Great Britain

0017-9310/93 $6.00 + 0.00

An experimental investigation on natural convection of air in a vertical channel

A. LA PICA, G. RODONÒ and R. VOLPES
Dipartimento di Energetica, Università di Palermo,
Viale delle Scienze, 90128 Palermo, Italy

(*Received* 4 *April* 1991)

Abstract—The free convection of air in a vertical channel is studied experimentally in a laboratory model of height $H = 2.6$ m and rectangular cross-section $b \times s$, with $b = 1.2$ m and the channel width s variable. One of the channel walls is heated with a uniform heat flux. Tests are made with different values of channel gap and heating power ($s = 7.5, 12.5, 17$ cm; $q_c = 48$–317 W m^{-2}). On the basis of the results two empirical formulae are found, giving Nu and Re as functions of Ra and the geometrical parameter s/H:

$$Nu = 0.9282\, Ra^{0.2035}(s/H)^{0.8972}; \quad Re = 0.5014\, Ra^{0.3148}(s/H)^{0.418}.$$

The mathematical form of these relationships reproduces other previously published formulae, valid for simpler geometries, though with different constants.

INTRODUCTION

NATURAL convection processes are often used in the building industry as well as in some nuclear technologies, in electronic circuit board cooling, and many other fields. The literature on this subject is quite a rich one, as a consequence of the strong dependence of the convection process upon many thermophysical and geometrical variables. Published studies deal, in general, with the simplest geometries: a single flat plate, for example [1–4], two parallel plates or a vertical channel of uniform cross-section [5–12], and so on. Boundary conditions are given as uniform wall temperature or uniform heat flux, or a combination of the two kinds of conditions.

Among experimental researches, an extensive investigation reported by Sparrow *et al.* [9, 10, 13, 14] on free convection in converging, diverging and parallel channels, placed in upright and inclined positions, is particularly noticeable for the variety of channel shapes and inclinations. However, the geometrical configuration of a channel with straight walls is still a rather simplified one, in comparison with some geometries actually encountered in practice. For this reason some authors have extended their interest to somewhat more complicated geometries [15–17].

The work reported here is intended to contribute to the research on the topic with a study of the free convective flow of air through a straight, vertical channel with uniform, rectangular cross-section, connected at the top and bottom ends to a plenum chamber through short horizontal ducts having the same cross-section as the main channel. One of the walls forming the vertical channel is heated with a uniform and constant heat flux, while the other walls are approximately adiabatic.

EXPERIMENTAL APPARATUS

The tests were run in an experimental apparatus (Figs. 1 and 2) placed between two laboratory rooms in a university building (Fig. 3). The model had a width of 1.2 m and a height of ≈ 3 m; it was inserted in the partition wall between the two rooms, one of which (A_1) was used as a plenum chamber to recirculate the air. The partition wall, expressly installed for this research, had a light structure with a plywood plate and an 8 cm layer of mineral wool. The chamber A_1 could be entered from room A_0 through a small door for instrumentation servicing; apart from this, the plenum chamber had no door, window or any other opening [18].

The channel gap was variable in the range 7.5–17 cm. One of the two wider walls forming the channel (referred to as the hot wall in the following) was heated electrically with a nearly uniform heat flux distribution; the other one (the cold wall) was not heated, while it allowed a limited heat loss to the room A_0. The side walls were thermally insulated by layers of mineral wool.

The top and bottom horizontal ducts were simply constructed from wood plates 1.5 cm thick. Each duct had a length of 20 cm and the same cross-section as the main channel, i.e. a width of 1.2 m and a variable height. The variation of the section was obtained by displacement of a movable plate placed in the duct as a wall.

The hot wall surface was heated by electrical resistance. The wall surface was divided into three equal sections (1200 mm × 867 mm) where three plates of electronic circuit board of the same size were applied. Each plate was chemically engraved as to form a long copper resistor 35 μm thick and 8.8 mm wide, distri-

NOMENCLATURE

b	width of walls
c_p	isobaric specific heat of air at inlet
g	acceleration of gravity
G	mass flow rate
Gr	Grashof number based on channel height, $g\beta q_a H^4/kv^2$
$\bar{h}$	overall convective coefficient as defined by equation (1)
H	channel height
k	thermal conductivity of air at inlet
n	number of test runs
Nu	Nusselt number, $\bar{h}s/k$
Pr	Prandtl number, $c_p\mu/k$
q_a	convective heat flux (power transferred by convection to air per unit area)
q_e	electrical heat flux (heat power generated per unit area)
Ra	Rayleigh number, $Gr\,Pr$
Re	Reynolds number, $\bar{u}s/v$
s	channel gap (distance between hot wall and cold wall)
S	surface area of the hot wall
t_w	hot wall surface mean temperature
t_{mc}	mean temperature of the air in the channel, $(t_1+t_2)/2$
t_1	air mixing temperature at the inlet section of the channel
t_2	air mixing temperature at the outlet section of the channel
$\bar{u}$	inlet mean air velocity
W_a	convective power transferred to the air flow.

Greek symbols

β	isobaric coefficient of thermal expansion of air at inlet
μ	viscosity of air at inlet
v	kinematic viscosity of air at inlet.

buted all over the plate surface, with an electrical resistance of $\approx 7.9\ \Omega$ at 20°C. The three electrical circuits were connected in parallel and independently powered at low voltage a.c. by autotransformers. These were manually set in order to obtain equal values of power dissipated in the three circuits. Independent control of heat fluxes generated in the circuits was possible this way, even with some non-uniformity of temperature along the wall. The circuit boards were glued to the wall with an adhesive capable of withstanding temperatures over 90°C.

The hot wall was a rigid sandwich panel made of

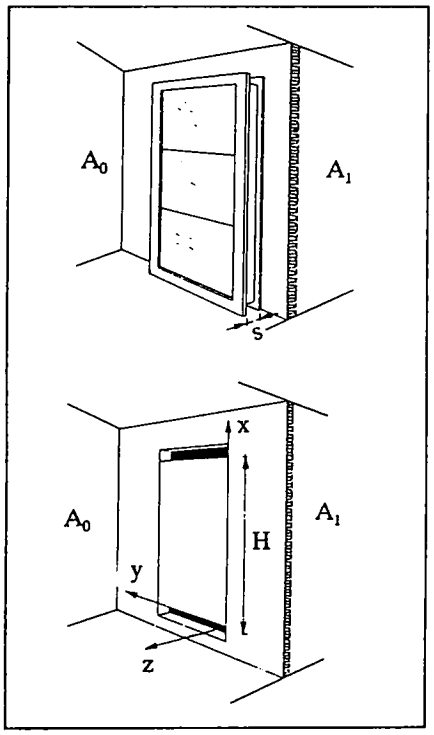

FIG. 1. Sketches of the model. Upper: view from room A_0; lower: view with the vertical channel taken out.

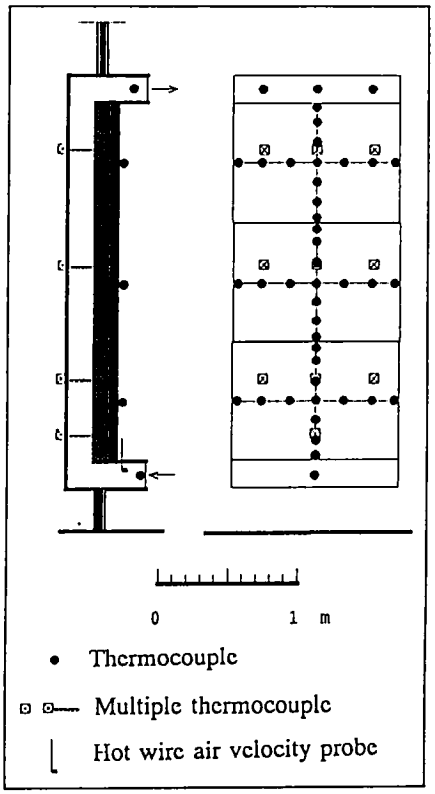

FIG. 2. View and section of the experimental model.

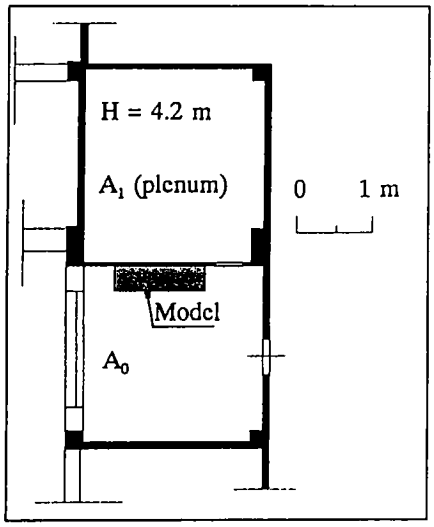

FIG. 3. Plan of rooms A_0 and A_1.

three layers of plaster–cardboard plate, one layer of mineral wool and a layer of honeycomb thermal insulator. The panel had a thickness of 115 mm, a specific mass of 30 kg m^{-2} and a specific thermal conductance of 0.62 W m^{-2} K^{-1}.

The cold wall was made of a 6 mm thick glass plate held by a wooden frame, which was designed to permit variations in the gap s between the two walls by simply changing a spacer. The inner side of the glass was silvered, in order to minimize the radiant heat flux from the hot wall. Ten small holes in the glass plate (Fig. 2) permitted air temperature measurements with a multiple thermocouple probe. The latter was a comb-shaped multiple probe (Fig. 4), equipped with 11 thermocouples made of 70 μm diameter wires. These holes were plugged with plastic elements when no probe was inserted. These plugs, as well as the multiple probe, were flush with the inner surface of the plate, in order to minimize the flow disturbances.

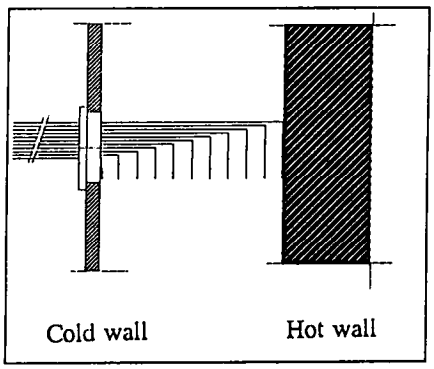

FIG. 4. Multiple thermocouple probe for air temperature measurements across the convective flow.

The heat flux generated on the hot wall surface was partly transmitted by convection to the air while the rest flowed across the wall itself to the ambient A_1. However, the latter part was only a small fraction of the total heat flux because of the low wall transmittance in comparison with the convective coefficient to the air. Therefore imposing the condition of uniform heat flux generation all along the wall surface turned out as a condition of convective heat flux nearly uniform on the hot wall surface.

Temperature measurements were made at the hot wall surface, on the cold glass, at the air inlet and outlet, in the air in both A_0 and A_1 rooms, at the A_1 side surface of the hot wall and in the air flow inside the vertical channel.

The hot wall surface temperature showed large variations along the lowest 80 cm, while it was fairly uniform in the second half of the height.

The temperature distribution with height in the room A_1 was also measured with two different values of heating power (about 100 and 250 W m^{-2}). In the worst case the average temperature gradient along the channel height was not greater than 0.6 K m^{-1}. Instead, a hot air layer was found in the room above the level of the channel outlet, that could exert no influence on the air flow in the channel.

All temperature data were taken by means of copper–constantan thermocouples and logged through a computer-driven multi-channel data acquisition unit.

The air flow rate in the channel was determined by measuring the air velocity at the inlet section by a hot wire constant-current anemometer (DISA mod. 55D01) equipped with a 5 μm diameter, 1.2 mm long, tungsten wire. The hot wire probe, mounted on a carriage, sweeped all the inlet section taking 96 air velocity data at as many points equally spaced.

The instrument calibration was temperature-compensated numerically by means of measured values of the inlet air temperature [19]. The inlet air temperature, measured with a single thermocouple, was assumed uniform throughout the section. The mass flow rate was calculated on the basis of the mean air velocity computed with these data.

The air temperature distribution across the outlet section was explored in two different operating conditions (heating power 100 and 250 W m^{-2}). Dispersion of temperature data all over the section was not greater than 16% of the temperature increment $(t_2 - t_1)$, with a standard deviation of 0.66°C. On this basis, the arithmetic mean of temperature data given by thermocouples placed at three different locations in the outlet section was taken as representative of the mixing air temperature t_2.

TESTS AND RESULTS

The scope of the study was to investigate the free convective air flow in the channel in several operating

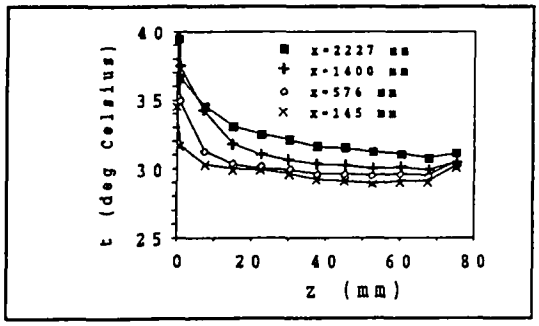

FIG. 5. Temperature profiles across the channel. $s = 7.5$ cm; $q_c = 48$ W m^{-2}.

conditions. To this aim, tests were run with different values of specific heat flux generation on the wall (in the range 48–317 W m^{-2}) and with three different values of channel gap (7.5, 12.5 and 17 cm).

The tests were done by fixing the electrical power, waiting until stabilization of steady state conditions, then taking all measurements.

The data collected allowed computation of the air mass flow rate, the convective thermal power and the overall convection coefficient at the hot wall surface. A consistency check was possible by balancing electrical power vs all power losses by convection and through the channel walls. This was made possible by the temperature measurements taken at the outer sides of the walls and by making adequate assumptions for convective coefficients towards A_0 and A_1.

An example of temperature profiles measured across the air channel is shown in Fig. 5, referring to four measurement stations placed at wall mid-span and four different heights.

The Rayleigh number calculated for all the cases tested, based on convective heat flux and channel height, ranges between 7.0×10^{12} and 5.3×10^{13}. A turbulent regime of the air flow is clearly recognizable from the fluctuations of temperature in a range of about 5°C observed at the outlet section. Figure 6

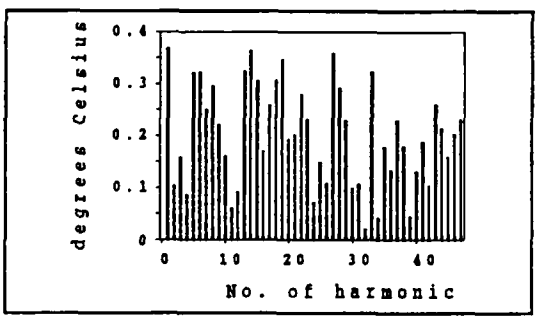

FIG. 6. Fourier analysis of outlet air temperature.

presents the Fourier analysis of 94 temperature values measured in a 235 s period of time with a 2.5 s time interval between measurements. The signal components given by the analysis are distributed in the whole frequency range considered; no characteristic frequency is prevailing, as in the turbulent flow pattern described by Mahajan and Gebhart [2].

Application of the criterion for predicting the end of transition proposed by Mahajan and Gebhart [2] also indicates a fully turbulent flow in all the cases studied.

The most significant results of the measurements are summarized in Table 1. Here the geometrical parameters, the heating power, the wall and air temperatures, the air mass flow rate and the convective power are presented for each of the 17 tests run. The overall convective coefficient $\bar{h}$:

$$\bar{h} = \frac{W_a}{S(t_w - t_{mc})} \tag{1}$$

is also presented, as resulting from the following heat balance:

$$W_a = c_p G(t_2 - t_1) \tag{2}$$

where the heat flux across the glass wall is neglected. In all cases studied, the convective coefficient $\bar{h}$ ranges between 5.1 and 8.4 W m^{-2} K^{-1} with a slight tendency to increase when heat flux increases.

DATA CORRELATION

Some relevant non-dimensional groups are calculated and presented in Table 1: *Re*, *Nu*, *Gr*. As a geometric non-dimensional parameter the ratio s/H is used to characterize the model shape. Correlations among these non-dimensional parameters are presented in the following.

The mean convective coefficient is given in non-dimensional form by the Nusselt number *Nu*. A dependence law of Nusselt number upon Rayleigh number and aspect ratio was searched for, assuming the mathematical form

$$Nu = B\, Ra^m\, (s/H)^p \tag{3}$$

on the basis of empirical equations reported in the literature for other cases of natural convection. Application of the method of least squares to the logarithms of *Nu*, *Ra* and s/H has yielded

$$Nu = \frac{\bar{h}s}{k} = 0.9282\, Ra^{0.2035}\, (s/H)^{0.8972}. \tag{4}$$

Equation (4) is graphically represented by solid lines in Fig. 7; experimental data are indicated with symbols. Reproduction of data is satisfactory: the maximum deviation of *Nu* is 9%; the standard error σ_{Nu} is 1.7. The correlation coefficient is 0.9985.

Similarly, the Reynolds number *Re* is used as a non-dimensional expression of the air velocity. To cor-

Table 1. Summary of experimental data

Quantity	Unit	s = 7.5 cm; s/H = 28.8 × 10^{-3}						s = 12.5 cm; s/H = 48 × 10^{-3}						s = 17 cm; s/H = 65.3 × 10^{-3}					
Measured variables																			
Electrical heating power per unit area, q_e	W m^{-2}	48	96	144	192	240	288	307	144	192	240	288	317	48	96	192	240	317	
Air inlet temperature, t_1	°C	28.6	27.1	29.3	27.3	24.9	25.8	30.5	21.5	22.6	22.8	23.5	21.8	23.2	20.7	20.9	21.5	22.2	
Air outlet temperature, t_2	°C	33.6	35.2	40.2	40.1	40.0	43.2	49.0	29.8	32.2	34.7	36.4	35.9	26.4	25.7	29.10	31.2	34.0	
Mean wall temperature, t_w	°C	39.1	45.5	54.7	58.7	62.6	70.2	76.9	44.4	51.2	57.3	63.7	64.3	32.7	37.2	49.9	55.9	64.8	
Inlet mean air velocity	m s^{-1}	0.27	0.35	0.36	0.43	0.44	0.46	0.49	0.28	0.31	0.34	0.35	0.36	0.16	0.20	0.23	0.26	0.29	
Calculated variables																			
Mass flow rate, G	g s^{-1}	28.5	36.6	37.5	45.1	46.7	48.8	51.5	50.3	56.1	60.7	63.2	65.2	38.9	48.3	57.1	63.8	70.2	
Convective power per unit area, q_a	W m^{-2}	46.0	96.0	132.0	186.0	227.0	274.0	307.0	135.0	173.0	233.0	263.0	296.0	40.0	78.0	151.0	199.0	267.0	
Overall hot wall-to-air convective coefficient, $\bar{h}$	W m^{-2} K^{-1}	5.8	6.6	6.6	7.4	7.5	7.7	8.3	7.2	7.3	8.2	7.8	8.4	5.1	5.6	6.1	6.8	7.3	
Non-dimensional parameters																			
Nusselt number (Nu)		16.5	19.0	18.7	21.2	21.7	22.0	23.4	34.8	35.2	39.3	37.5	40.4	33.4	36.7	40.0	44.4	47.8	
Reynolds number (Re) × 10^{-3}		1.28	1.65	1.68	2.03	2.12	2.21	2.30	2.31	2.56	2.77	2.88	2.99	1.78	2.22	2.62	2.93	3.22	
Grashof number (Gr) × 10^{-12}		10.3	22.1	29.3	42.8	54.7	64.8	66.7	34.5	43.6	58.3	64.9	75.6	9.97	20.3	39.2	51.2	67.7	
Prandtl number (Pr) × 10^{3}		706.29	706.42	706.22	706.40	706.55	706.50	706.09	706.64	706.63	706.62	706.61	706.64	706.62	706.64	706.64	706.64	706.63	
Rayleigh number (Ra) × 10^{-12}		7.30	15.6	20.7	30.2	38.7	45.8	47.1	24.4	30.8	41.2	45.9	53.4	7.04	14.3	27.7	36.2	47.8	

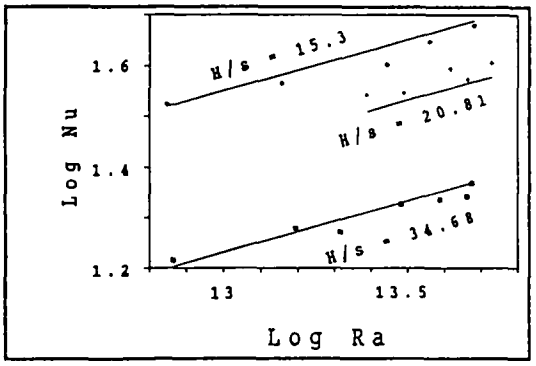

FIG. 7. Nusselt number vs Rayleigh number and s/H. Solid lines represent equation (4).

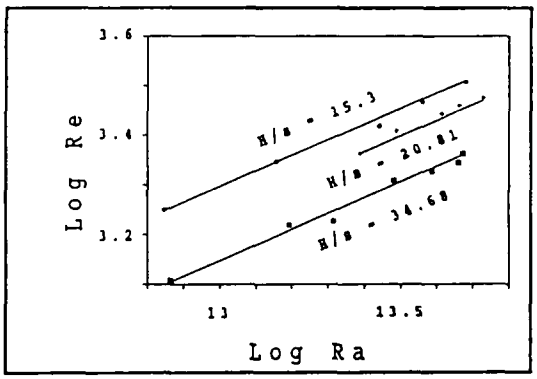

FIG. 8. Reynolds number vs Rayleigh number s/H. Solid lines represent equation (5).

relate the experimental values of the Reynolds number the following equation has been found:

$$Re = \frac{\bar{u}s}{\nu} = 0.5014\, Ra^{0.3148}\,(s/H)^{0.418} \qquad (5)$$

that is represented in Fig. 8. The maximum deviation is here 5%; the standard error σ_{Re} is 51. The correlation coefficient is 0.9998.

The correlation evaluation parameters are still satisfying if all constants in equations (4) and (5) are rounded to the third significant digit. In this case the following values for maximum deviation, standard error and correlation coefficient are obtained:

$$\delta_{Nu,\max} = 11\%; \quad \sigma_{Nu} = 1.8; \quad R_{Nu} = 0.9984;$$

$$\delta_{Re,\max} = 6\%; \quad \sigma_{Re} = 55; \quad R_{Re} = 0.9997.$$

CONCLUSIONS

Some convective heat exchangers may have a configuration similar to the one studied here; for example the Trombe wall, the well-known device used to collect solar radiation for room heating. Other free-convection heat exchangers, of different shape, slope, inlet and outlet geometries, etc., may also be simulated, more or less accurately, by the same model.

Equations (4) and (5), expressing the Nusselt and Reynolds numbers as functions of Rayleigh number and channel geometry, are the main result of the research.

The Nusselt number, as given by equation (4), depends upon the Rayleigh number to the power 0.2035 ($\approx 1/5$) and the shape factor s/H to the power 0.8972. This conclusion deviates from other known laws on natural convection (Elenbaas, Sparrow), that state a dependence on Ra to the power 1/3–1/4 and on s/H to the same power as Ra. Such discrepancies can be attributed to the particular geometry of the model tested, whose extremity ducts and 90° elbows are likely to exert a strong influence on the fluid flow structure and, consequently, on convective heat exchanges.

The mathematical shape of the formula found for Re, equation (5), is of the same type. This result is of interest, since no published formula of this kind for Re has been found in the literature by the authors.

Acknowledgements—The research was supported by the Italian government with funds 'MPI-60% (1988)'.

REFERENCES

1. J. Coutanceau, Convection naturelle turbulente sur une plaque verticale isotherme. Transition, échange de chaleur et frottement pariétal, lois de répartition de vitesse et de température, *Int. J. Heat Mass Transfer* **12,** 753–769 (1969).
2. R. L. Mahajan and B. Gebhart, An experimental determination of transition limits in a vertical natural convection flow adjacent to a surface, *J. Fluid Mech.* **91**(1), 131–154 (1979).
3. R. G. Bill, Jr. and B. Gebhart, The development of turbulent transport in a vertical natural convection boundary layer, *Int. J. Heat Mass Transfer* **22,** 267–277 (1979).
4. T. Tsuji and Y. Nagano, Characteristics of a turbulent natural convection boundary layer along a vertical flat plate, *Int. J. Heat Mass Transfer* **31,** 1723–1734 (1988).
5. W. Elenbaas, Heat dissipation of parallel plates by free convection, *Physica* **IX**(1), 1–28 (1942).
6. W. Elenbaas, The dissipation of heat by free convection [at] the inner surface of vertical tubes of different shapes of cross-section, *Physica* **IX**(8), 865–874 (1942).
7. A.-M. Dalbert, F. Penot et J. L. Peube, Convection naturelle laminaire dans un canal vertical chauffé à flux constant, *Int. J. Heat Mass Transfer* **24,** 1463–1473 (1981).
8. A. Bar-Cohen and W. M. Rohsenow, Thermally optimum spacing of vertical, natural convection cooled, parallel plates, *ASME J. Heat Transfer* **106,** 116–123 (1984).
9. L. F. A. Azevedo and E. M. Sparrow, Natural convection in open-ended inclined channels, *ASME J. Heat Transfer* **107,** 893–901 (1985).
10. E. M. Sparrow and L. F. A. Azevedo, Vertical-channel natural convection spanning between the fully-developed limit and the single-plate boundary-layer limit, *Int. J. Heat Mass Transfer* **28,** 1847–1857 (1985).
11. S. H. Kim, N. K. Anand and W. Aung, Effect of wall conduction on free convection between asymmetrically heated vertical plates: uniform wall heat flux, *Int. J. Heat Mass Transfer* **33,** 1013–1023 (1990).
12. T. R. Borgers and H. Akbari, Free convective turbulent flow within the Trombe wall channel, *Sol. Energy* **33,** 253–264 (1984).
13. E. M. Sparrow, R. Ruiz and L. F. A. Azevedo, Experimental and numerical investigation of natural convection in convergent vertical channels, *Int. J. Heat Mass Transfer* **31,** 907–915 (1988).
14. E. M. Sparrow and R. Ruiz, Experiments on natural convection in divergent vertical channels and correlation of divergent, convergent and parallel-channel Nusselt numbers, *Int. J. Heat Mass Transfer* **31,** 2197–2205 (1988).
15. J. R. Dyer, Natural-convective flow through a vertical duct with a restricted entry, *Int. J. Heat Mass Transfer* **21,** 1341–1354 (1978).
16. S. A. M. Said and R. J. Krane, An analytical and experimental investigation of natural convection heat transfer in a vertical channel with a single obstruction, *Int. J. Heat Mass Transfer* **33,** 1121–1134 (1990).
17. M. A. I. El-Shaarawi and M. A. Al-Nimr, Fully developed laminar natural convection in open-ended vertical concentric annuli, *Int. J. Heat Mass Transfer* **33,** 1873–1884 (1990).
18. A. La Pica, G. Rodonò, R. Volpes, Apparato per lo studio sperimentale della convezione libera entro un canale verticale, *Quad. Dip. di Energetica Univ. di Palermo* no. 1. Palermo (1989).
19. P. Barrera, A. La Pica, G. Rodonò, R. Volpes, Sulla taratura delle sonde anemometriche a filo caldo in aria a bassa velocità e temperatura variabile, *Atti del 3° congresso nazionale dell'UIT*, Palermo, pp. C3–C22 (1985).